APOLLO MISSION EXPERIENCE*

Herman J. Schaefer
Naval Aerospace Medical
Research Laboratory
Pensacola, Florida

The preceding papers have drawn a detailed picture of the natural radiation environment in space. It is the purpose of this presentation to proceed to a discussion of the dosimetric implications for manned space missions. In other words, it is to be analyzed what the radiation field behind the heavy shielding of a manned space vehicle on a near-Earth orbital or a lunar mission will look like and how it compares with actual exposure levels recorded on the Apollo missions. In line with this objective, emphasis will shift from flux densities and energy spectra of the incident radiation to absorbed doses and dose equivalents as they are recorded within the ship preferably at locations close to the crew members.

On all missions, the Apollo astronauts were equipped with a number of different active and passive dosimeters intended for a twofold purpose. On the one hand, the astronauts should be able to carry out, at any time, in-flight readings of instantaneous radiation levels. On the other hand, accurate data on accumulated absorbed doses and dose equivalents were to be collected. From the radiation safety viewpoint, the latter data, i.e., the grand total mission doses, are of main interest. Turning to this information we see in Table I a tabulation of the grand total mission doses as they were recorded with TLD dosimeters carried by the astronauts under their space suits. Taken at face value, the picture looks very reassuring. The highest dose, encountered on Apollo XIV, remains under one rad. Another interesting fact seen from Table I is that the mission dose shows no correlation at all to mission duration, i.e., to exposure time in space. The reason for this lack of correlation is to be sought in the greatly different trajectories through the inner radiation belt as will be discussed in detail later.

If we attempt to convert the mission doses in Table I to dose equivalents, the situation becomes more complicated. Radiation exposure in space is mainly due to nuclear particles of a large variety of different kinds each, in turn, covering a broad energy spectrum. As a consequence, the Linear Energy Transfer (LET) spectrum is extremely complex. In fact, it extends from minimum ionization to values exceeding by more than a factor of 10 the highest LET obtainable from terrestrial sources.

The most accurate and sensitive LET analyzer is nuclear emulsion. In view of the very wide LET spectrum encountered in space, combinations of different emulsion sensitivities are usually applied in order to ensure sustained resolution over the full LET scale. The details of the nuclear emulsion technique as it applies to measuring the astronauts' radiation exposure have been described repeatedly throughout the past ten years when we monitored the Mercury, Gemini, and Apollo flights. Therefore, we can proceed directly to the final result of the nuclear emulsion analysis for a particular mission and present in Table II a breakdown of the total dose on the first lunar landing mission Apollo XI. It is seen that the make-up of the total exposure is indeed quite complex. Problems arise especially if one tries to establish Quality Factors (QF's) for the conversion of the various dose fractions from absorbed doses to dose equivalents.

Table I

Average Doses on Apollo Missions

Mission	Type	Launch Date	Duration, Hours	Mission Dose, millirads
Apollo 7	Earth-orbital	11 Oct 1968	260	160
Apollo 8	Circumlunar	21 Dec 1968	147	160
Apollo 9	Earth-orbital	3 Mar 1969	242	200
Apollo 10	Circumlunar	18 May 1969	192	470
Apollo 11	Lunar Landing	16 Jul 1969	195	180
Apollo 12	Lunar Landing	14 Nov 1969	245	577
Apollo 13	Circumlunar	11 Apr 1970	143	237
Apollo 14	Lunar Landing	31 Jan 1971	216	[~ 900 est.]

Table II

Components of Mission Dose on First Lunar Landing Mission Apollo XI

Component	Absorbed Dose, millirad	Dose Equivalent, millirem
Protons	150	220
Stars	15	94
Fast neutrons	~1	~12
Heavy nuclei	5	46
Electrons and gamma rays	~30	~30
Total	201	402

*The paper is based on measurements carried out as contract work for the Manned Spacecraft Center, NASA, Houston, Texas.

No special difficulties exist with regard to the proton dose. By far the largest part of the dose results from trapped protons in the radiation belt. On standard near-Earth orbital missions such as the preparatory missions Apollo VII and IX, trapped protons are encountered in repeated passes through the South Atlantic Anomaly. On lunar missions, they are encountered in two complete traversals of the radiation belt on translunar and trans-Earth injection. Since the angle of inclination of the plane of the geomagnetic equator to the plane of the coplanar orbits of the Moon and the vehicle around the Earth varies continuously on a daily and monthly cycle, the geomagnetic trajectory through the radiation belt varies from crossing to crossing. Sometimes the trajectory traverses the inner belt more peripherally, sometimes more centrally. The two crossings on the Apollo XII mission are typical in this respect as seen from Figure 1. Without carrying out any tabulation and adding of isoflux line values, one sees by inspection that the dose on the return trajectory from the Moon must have been disproportionately larger than on the way out.

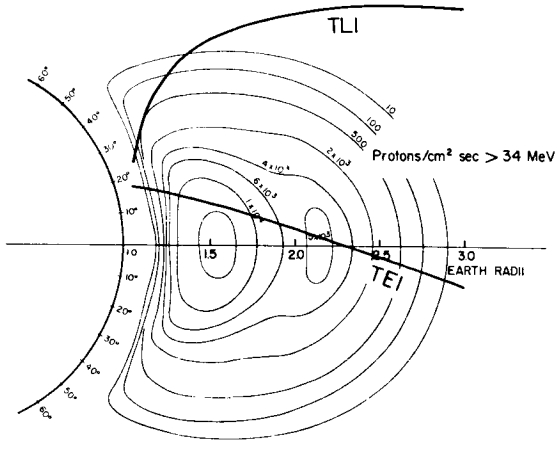

GEOMAGNETIC TRAJECTORIES OF TRANSLUNAR AND TRANS-EARTH INJECTION OF APOLLO XII MISSION Figure 1

Figure 1. Geomagnetic Trajectories of Translunar and Trans-Earth Injection of Apollo XII Mission

Energy spectrum and LET distribution of a proton flux traversing a nuclear emulsion can be established by track and grain count analysis. It was mentioned above that by flying emulsions of different sensitivities in the same pack, a sustained resolution for the entire energy scale from zero to relativistic energies can be achieved. Figure 2 shows the result of the combined evaluation of emulsions of three different sensitivities (Ilford G.5 and K.2 and Eastman Kodak NTA) in the radiation pack on Neil Armstrong's ankle on the first lunar landing mission Apollo XI. Dosimetrically the essential feature is that a substantial fraction of the total dose is produced by low-energy protons. Since these protons have short ranges the flux density depends sensitively on the local shield distribution and shows sizeable variations at locations with different slant or shadow shielding geometry within the vehicle.

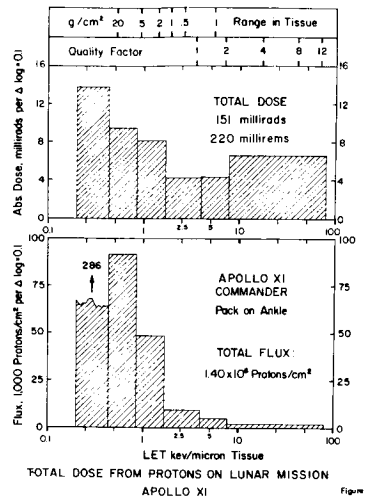

Figure 2. Total Dose from Protons on Lunar Mission Apollo XI

To what extent the shield distribution makes itself felt in directional effects of the population of enders, i.e., of protons reaching the end of their ionization ranges has been analyzed in detail on the unmanned missions Apollo IV and VI. These flights combined several traversals of the South Atlantic Anomaly with the two traversals of the core of the inner radiation belt when the vehicle swung out, on its last orbit, to an Apogee well beyond the inner belt. On Apollo VI with a total proton dose of 1.56 rad the density of enders in the emulsions reached a level which allowed a directional analysis in all three dimensions. Figure 3 shows the result of this analysis for a K.2 emulsion from one of two emulsion spectrometers flown on Apollo VI. It is clearly seen that there is a solid angle of minimum shield thickness within which eight times more proton enders arrive than within the solid angle of maximum shield thickness subtended by the heavy base of the command module and the heat shield.

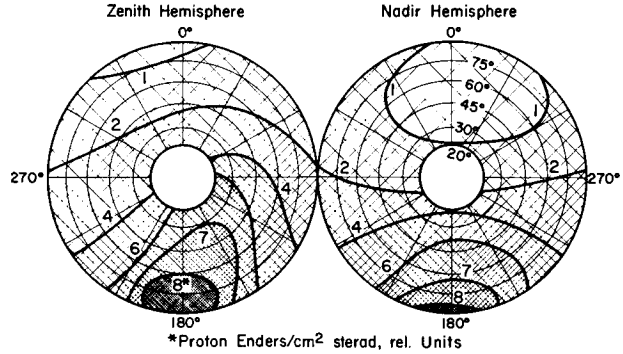

Figure 3. Directional Distribution of Proton Enders in Upper Chamber of Proton Spectrometer S/N5 Flown on Apollo VI

Radiobiologically more interesting are the large microdosimetric fluctuations of the proton dose reflecting the Poisson distribution of the fluence of low-energy protons. At first sight, one might expect that the spontaneous statistical fluctuations in the fluence of low-energy particles through small target volumes would entirely vanish in the much larger fluences of medium and high-energy protons. As far as fluences, i.e., mere particle numbers are concerned, this assumption is indeed correct. For the total dose, however, it is not. Since a low-energy proton traversing a small target volume contributes a substantially larger share to the total dose than a medium or high-energy particle, the local Poisson variations of the enders fluence show up quite strongly in the total dose. Figure 4 shows the quantitative aspects of the effect, again for the radiation pack on Neil Armstrong's ankle from which also the data presented in Figure 2 were taken. It should be emphasized that the dose distribution of Figure 4 hold for a comparatively large target volume comprising some 30 cells and that it pertains to the total dose. Since the fluctuations are exclusively due to low-energy particles they affect only the high-LET fraction of the total dose. Therefore, the corresponding Poisson variations of the dose equivalent must be substantially larger than those of the absorbed dose shown in Figure 4.

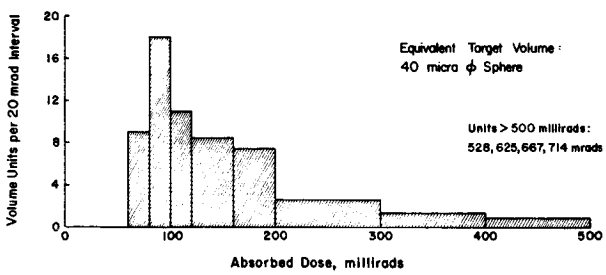

MICRODOSIMETRIC DISTRIBUTION OF PROTON DOSES IN ILFORD G.5 EMULSION ON APOLLO XI

Figure 4. Microdosimetric Distribution of Proton Doses in Ilford G.5 Emulsion on Apollo XI

It should be pointed out that the uneven distribution of the local dose due to the Poisson variations of the fluence of low-energy protons is superimposed upon the ununiformity of the energy dissipation in the microstructure of tissue due to the dense columns of ionization of the individual particles which finds its dosimetric expression in the LET. The Poisson variations of the fluence added to the latter ununiformity is bound to lead to a further increase of the biological effectiveness which is not adequately expressed in the conventional QF/LET relationship as set forth by the International Commission on Radiological Protection (ICRP). It would seem an important task to design radiobiological experimentation which would furnish quantitative data on this peculiar characteristic of proton radiation in space.

A peculiar component of any radiation exposure in space is the dose from disintegration stars in tissue. The name star stems from the characteristic microscopic appearance of nuclear disintegrations in nuclear emulsion. Well known are the spectacular multipronged stars from disintegrations of the heavy elements silver and bromine in emulsion. Obviously, they cannot occur in tissue. However, stars with smaller prong numbers originate from disintegrations of carbon, nitrogen, and oxygen atoms in the gelatin matrix. Since gelatin is a tissue-equivalent material, these stars allow a direct determination of the tissue dose from the star phenomenon. The additional star production in gelatin makes itself felt in a steepening of the slope of the integral prong spectrum in the region of $Z = 6$ to 8 according to the heaviest constituent elements of gelatin. Figure 5 shows the integral prong spectrum for Apollo XI based on a total of 1395 analyzed stars in the K.2 emulsions. The change in slope in the region of 6 to 8 prongs is clearly seen.

The star prongs represent protons and alpha particles of low energies coming to rest locally in tissue. Accordingly, the LET spectra of star particles center on rather high values. In the Bragg peaks of protons and alpha particles, the LET reaches 90 and 270 kev/micron T, respectively. Corresponding, the mean QF for the star dose is quite high and the dose equivalent substantially larger than the absorbed dose. As indicated in Table II, the star count on Apollo XI leads to an absorbed dose of 15 millirad and a dose equivalent of 94 millirem.

Closely connected to the star phenomenon is the neutron dose. Neutrons are generated in disintegration stars in the same way as protons and alpha particles. However, since neutrons themselves do not ionize, their paths do not appear as visible prongs originating in the star center hence the neutron dose cannot be determined from the star count. The bulk of the neutron dose in space is due to fast neutrons. In the hydrogen content of the gelatin of nuclear emulsion, fast neutrons release recoil protons which in turn produce short tracks that can be identified easily. Also produced are heavy recoils with extremely short ranges that disappear completely in the comparatively heavy background of emulsions exposed to radiation in space. However, since the proton recoil dose is by far the larger dose contribution, the error due to omission of the heavy recoils is small.

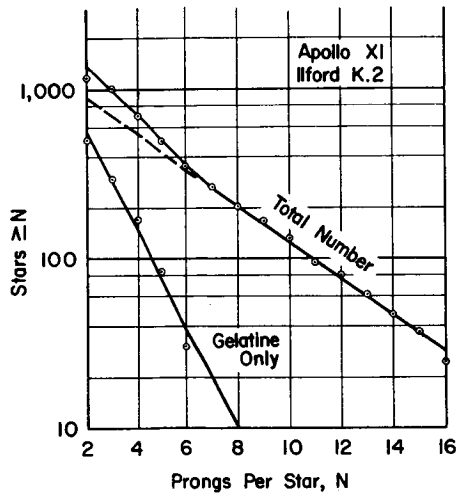

INTEGRAL PRONG SPECTRUM OF STAR POPULATION IN ILFORD K.2 EMULSIONS ON APOLLO XI

Figure 5. Integral Prong Spectrum of Star Population in Ilford K.2 Emulsions on Apollo XI

A much more serious handicap in the determination of the neutron dose results from the large population of trapped protons. Since the spectrum of these protons reaches all the way down to zero energy with a substantial flux fraction being of short range, the neutron recoil protons are masked by large numbers of true primary protons. The only clue for direct identification of a recoil proton is the test whether its track begins and ends in the emulsion. Naturally, this criterion allows only the establishment of a lower limit of the neutron dose since an unknown fraction of tracks ending in the emulsion yet entering from the outside represents recoils released in the material surrounding the emulsion. Within limitations, additional clues can be derived from the range distributions of enders and suspended tracks. However, this analysis is costly in time because it requires evaluation of large track populations for statistical significance. It is beyond the scope of this presentation to discuss the method of spectral discrimination in more detail.

Dosimetrically, the failure of the emulsion method to furnish direct clues as to the origin of low energy protons is irrelevant as long as tissue equivalence is preserved, i.e., the assurance is given that the neutron recoils entering the emulsion from the outside originate in tissue equivalent material. If this condition is fulfilled the total "proton" dose as it follows from the track and grain count analysis represents the correct sum of the doses from galactic and trapped protons and from neutrons. Expressed in terms of Table II this means that the neutron dose is underrated but the missing part, although unknown as to its magnitude, is correctly contained in both the absorbed dose and the dose equivalent of the proton component.

The last component of the mission dose to be discussed is the most difficult and controversial: the dose from galactic heavy primaries. All through the years when we flew nuclear emulsions on the Mercury and Gemini missions, we kept a wary eye on the heavy tracks that were interspersed as infrequent events among the dense populations of proton tracks. The picture changed dramatically when we examined the emulsions from the first circumlunar mission Apollo VIII and compared the counts to those from the standard near-Earth orbital mission Apollo VII. We had been aware than in deep space outside the magnetosphere flux densities of heavy nuclei should be substantially higher because the energy spectrum would extend to much lower energies in the absence of any geomagnetic cutoff. We had estimated that the flux densities should increase by about a factor of 2.5. What we actually found was a sixfold increase. Table III shows a comparison of the flux densities on the two missions. Because of the substantially higher flux density in deep space, heavy nuclei in emulsions from lunar missions are no longer occasional events, but appear quite frequently in the emulsion scan, sometimes as doublets and triplets in the same microscopic visual field at high power.

Table III

Flux Densities of Heavy Primaries on Earth Orbital Mission Apollo VII and Circumlunar Mission Apollo VIII

Z-Class	Nuclei/(cm^2 24 hrs.) Apollo VII	Apollo VIII
3-9	24.6	148
10-20	16.5	99
21-30	2.1	12.6

Radiobiologically, the higher fluxes of heavy primaries on deep space missions do not constitute the main reason for concern. As far as tissue damage is concerned the extension of the spectrum to lower energies in the absence of a geomagnetic cutoff and the associated extension of the LET spectrum to substantially higher values weigh much more heavily. Within the magnetosphere, the cutoff effect excludes low-energy primaries completely. As a consequence, the very high LET values in the terminal sections of heavy nuclei tracks near or in the Bragg peak are not encountered at all on standard near-Earth orbital missions of low inclination. Heavy nuclei enders or thindowns do reach the Earth in the polar regions, but we have never seen any on the Mercury and Gemini missions. The first thindowns appeared on the first deep space mission, the circumlunar flight of Apollo VIII.

The quantitative relationships governing flux densities of heavy primary thindowns within and outside the magnetosphere are presented in Figure 6. It shows the incident and local differential range spectra for the heaviest component of the Z spectrum, the iron group (Z = 24 to 30), for solar maximum and minimum. The local spectra show fractional flux densities of nuclei escaping nuclear collisions and spending their kinetic energy entirely in ordinary ionizations down to zero energy. In other words, the local spectra show the thindown flux densities. With regard to the attenuation geometry, one has to realize that for a parallel beam the indicated thindown flux densities would occur at depth R in a target exposed to the incident spectrum. The essential feature of Figure 6 is the two vertical lines indicating the geomagnetic cutoff ranges for 30° and 40° latitude. These cutoff values mean that the flux density is zero for both the incident and local spectrum for the entire range scale below the cutoff values. Comparing the flux densities of the incident and local spectra for a given range to the right of the cutoff ranges, one immediately sees that for the indicated sample latitudes the thindown fluxes are by more than a factor of 100 smaller than the incident fluxes. A quick estimate of thindown hit frequencies for a ten-day mission and the small target areas of the radiation packs flown on all manned missions shows an extremely small hit probability and explains why no thindown hits have been observed so far on manned near-Earth orbital missions.

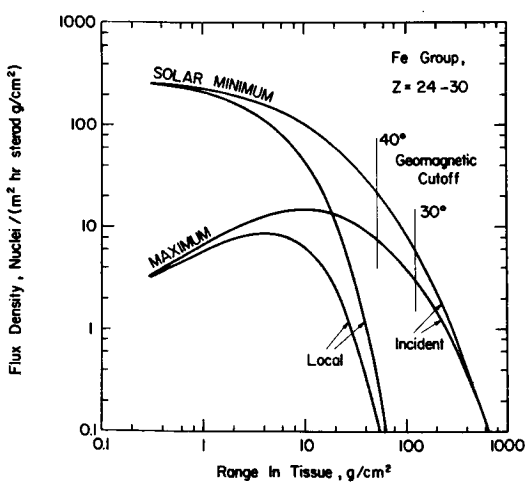

DIFFERENTIAL RANGE SPECTRA FOR IRON GROUP AT SOLAR MAXIMUM AND MINIMUM

Figure 6. Differential Range Spectra for Iron Group at Solar Maximum and Minimum

Heavy nuclei thindowns and near-thindowns constitute a radiation exposure which is well described with the term microbeam irradiation. Present knowledge in radiobiology is inadequate for a full understanding of the mode of action of this type of radiation exposure on living matter, especially as far as long-term effects from total body exposures at low dose rates are concerned. As the ICRP has stated expressly the conventional dosimetric concepts underlying the definitions of the rad and rem units are not applicable to microbeams. Satisfactory alternate methods of measuring the biological effectiveness of microbeam irradiation have not been proposed so far. Recent experiments of Tobias with alpha particle enders indicate that thindowns and near-thindowns of heavy primaries are responsible for at least two of the three different types of eye flashes experienced by the astronauts during periods of dark adaptation outside the magnetosphere on lunar missions.

In summing up the Apollo mission experience one can safely say that the natural environment of ionizing radiation in space did not impose constraints or create problems on any of the missions. While transitory radiation levels in passing through the radiation belt have reached several rads/hour accumulated doses remained well within official limits set for Radiation Workers. As no flare event of a large or medium size was encountered on any of the missions, no operational experience could be gained in that area. However, nobody is sorry about this particular issue remaining unsettled. Since we know very well that every flare event and the associated solar particle beam have their special characteristics with regard to time profile and configuration of the energy spectrum, not much could be learned anyway from a mission experiencing a major event. As far as the normal radiation environment in space is concerned, the single major source of exposure is the radiation belt. Since it dips down, in the South Atlantic Anomaly, so closely to the outer fringes of the atmosphere that near-Earth orbits of longer life times will have to encounter increased radiation levels, trapped protons will pose a problem for long or repeated duty cycles on skylabs and space platforms especially if an additional exposure from nuclear power sources has to be taken into consideration.